ISSN 1471-0498

DEPARTMENT OF ECONOMICS

DISCUSSION PAPER SERIES

Econometric Models of Climate Systems: The Equivalence of Two-Component Energy Balance Models and Cointegrated VARs

Felix Pretis

Number 750
June 2015

Manor Road Building, Oxford OX1 3UQ

Econometric Models of Climate Systems: The Equivalence of Two-Component Energy Balance Models and Cointegrated VARs

Felix Pretis*
Programme for Economic Modelling
Institute for New Economic Thinking
Oxford Martin School, University of Oxford

Abstract

Climate policy target variables including emissions and concentrations of greenhouse gases, as well as global mean temperatures, are non-stationary time series invalidating the use of standard statistical inference procedures. Econometric cointegration analysis can be used to overcome some of these inferential difficulties, however, cointegration has been criticised in climate research for lacking a physical justification for its use. Here I show that a physical two-component energy balance model of global mean climate is equivalent to a cointegrated system that can be mapped to a cointegrated vector autoregression, making it directly testable, and providing a physical justification for econometric methods in climate research. Doing so opens the door to investigating the empirical impacts of shifts from both natural and human sources, and enables a close linking of data-based macroeconomic models with climate systems. My approach finds statistical support of the model using global mean surface temperatures, $0-700$m ocean heat content and radiative forcing (e.g. from greenhouse gases). The model results show that previous empirical estimates of the temperature response to the doubling of CO_2 may be misleadingly low due to model misspecification.

JEL Classification: C32, Q54
Keywords: Cointegration; VAR; Climate; Energy Balance.

*Financial support from the Oxford Martin School and Open Society Foundations is gratefully acknowledged. I thank David Hendry, Robert Kaufmann, Janine Aron, Niels Haldrup, Søren Johansen, Eric Hillebrand, Bent Nielsen, Anders Rahbek, Katarina Juselius, Heino Bohn Nielsen, and Max Roser for helpful comments and suggestions. Contact: felix.pretis@nuffield.ox.ac.uk.

1 Introduction

Climate policy target variables including emissions and concentrations of greenhouse gases, as well as global mean temperatures are non-stationary time series invalidating the use of standard statistical inference procedures (Pretis & Hendry 2013, Kaufmann et al. 2013, Kaufmann & Stern 2002, D. I. Stern & Kaufmann 2000). Econometric cointegration analysis can be used to overcome the inferential difficulties resulting from stochastic trends when that is the only source of non-stationarity, and is applied to test whether there exist combinations of non-stationary variables that are themselves stationary (see Hendry and Juselius 2001 for an overview, Juselius 2011 for an application to climate data, and Kaufmann & Juselius 2013 for a paleo-climate analysis). Cointegration, however, has been criticised in climate research for lacking a physical justification. In turn, multiple-component physical energy-balance models (see Gregory et al. 2002, Held et al. 2010, Schwartz 2012, Pretis & Allen 2013) that model the ocean and atmosphere interactions have tracked global mean climate well while remaining analytically tractable, but are rarely formally tested as estimation is difficult due to the non-stationarity of observations. Here I show that two-component energy-balance models of global mean climate can be mapped to a cointegrated system, both making them directly testable, and providing a physical justification for econometric methods that account for data non-stationarity. This makes it possible to estimate a complete system model of global mean-climate model using econometric methods. Doing so opens the door to investigating the empirical impacts of shifts from both natural and human sources, and enables a coupling of climate systems with data-based macroeconomic models where econometric cointegration methods are the norm.

Stern (2013) argues for a new generation of models to better address the disconnect between climate and economics in integrated assessment models. The present paper provides the foundation for a new generation of empirical models linking economics and climate, providing a basis for models that are probabilistic, data-based, consistent with physical processes, and can be linked with socio-economic models due to the flexible nature of cointegrated systems.

Here I first show the mathematical equivalence of a two-component energy balance model to a restricted cointegrated system that can be mapped to a cointegrated vector autoregression (CVAR). This provides a system-based statistical framework in which an EBM can be estimated jointly (rather than one equation at a time) and therefore can be tested against observed data. Equally, this mathematical equivalence provides a physical basis for the application of econometric CVARs in climatology, and places the entire CVAR toolkit at the disposal of energy balance models coupled with empirical macroeconomic models.

Climate observations are predominantly non-stationary time series invalidating the use of standard statistical inference procedures such as ordinary least squares regression and simple correlations. This makes the estimation of parameters in EBMs from observations a challenge. Additionally, most statistical approaches which estimate model parameters from observations do not formally test whether the EBM is an appropriate model for the system but rather estimate one equation at a time. It is, however, exactly the system nature of two-component EBMs and the non-stationarity of the data that provides a useful property that allows EBMs to be tested against observations. As I will show, a two-component EBM is equivalent to a restricted CVAR

and this equivalence implies directly testable assumptions: if the model holds then the modelled series together form some stationary relations (cointegrate), restrictions across the estimated equations are not rejected, and individual parameters are statistically significant.

As an application, I estimate a two component EBM through the use of a CVAR and test it against the observational record. The approach here is highly simplified climatologically and takes the fast, mixed component as the atmosphere at the surface, while the slower component is proxied by the ocean heat content[1] from 0-700m. I find that tests against the statistical properties implied by the EBM do not reject the model. The time series form stationary relations (cointegrate) consistent with theory. Previous empirical estimates of equilibrium climate sensitivity (ECS) – the temperature response to a step-shift doubling of CO_2 concentrations – may be misleadingly low due to model mis-specification (e.g apparent through residual autocorrelation), partly induced by break-like volcanic aerosol forcing. Recursive estimates suggest that the recent slowdown in temperature increase, the "hiatus" (Kaufmann et al. 2011, Meehl et al. 2011, Watanabe et al. 2013), does not strongly affect the estimate of ECS. A simple forecasting exercise shows that the hiatus can be approximated through changes in radiative forcing and ocean heat uptake. The application illustrates the principal of empirical system-based estimation of a climate model, opening the doors to incorporating a macroeconomic model through the flexible structure of CVARs.

2 Two-Component Energy Balance Models

Two component energy balance models of climate are characterised by a mixed upper layer (the shallow ocean/atmosphere) with low heat capacity and a deeper ocean layer with higher heat capacity (Gregory et al. 2002, Held et al. 2010, Schwartz 2012). The upper, mixed (denoted by subscript m) component responds more quickly to perturbations (radiative forcing such as an increase in greenhouse gases[2]) and refers to the mixed layers of the atmosphere and shallow ocean. The deeper (denoted by subscript d) component responds slower and allows for delayed, recalcitrant warming (Held et al. 2010). In other words, if external forcing stopped and the system was in disequilibrium, high temperatures in the deep component would lead to a slow warming of the mixed atmosphere component (and vice versa). This energy balance model explicitly takes ocean-atmosphere interactions into account. A simple two-component EBM is given here as differential equations in (1)-(2). Let T_m be the temperature anomaly (deviations from steady state) for the mixed layer, C_m is the component heat capacity and F denotes radiative forcing. Heat capacity denotes the amount of energy needed to change the temperature of the component. Net heat flux denoting the net incoming energy is given by $Q = F - \lambda T_m$ where climate feedback is defined as λ, the change in downward net flux with temperatures T_m. The term λT captures the increasing outgoing long-wave radiation with

[1] The shallow depth implies the lower "slow" component will not be as slow as suggested in other studies.

[2] Together with many other factors (e.g. solar irradiance, reflective aerosols from volcanic eruptions, soot, etc.) the effect of GHGs is quantified through the concept of radiative forcing. In simple terms, this captures the change in energy in the atmosphere due to a change in concentration of a GHG or other factor. The radiative forcing effect, measured in watts per square meter (wm^{-2}), is calculated for the different forcing agents (e.g. GHGs, aerosols) and links the effect of the concentration of a gas on to temperatures.

increased temperatures.

The upper component of the model describes the changes in heat content relative to the steady state $C_m \frac{dT_m}{dt}$ as a function of net flux $F - \lambda T_m$ and the heat exchange H with the lower component:

$$C_m \frac{dT_m}{dt} = -\lambda T_m - H + F \tag{1}$$

The change in the heat content of the lower component $C_d \frac{dT_d}{dt}$ is given by:

$$C_d \frac{dT_d}{dt} = H \tag{2}$$

where C_d denotes the effective heat capacity of the deep component and T_d is the associated temperature anomaly. The heat exchange between the bottom and upper component is assumed to be proportional to the difference in temperatures:

$$H = \gamma(T_m - T_d) \tag{3}$$

Substituting this expression into the above equations yields the two component model as a system of two differential equations:

$$C_m \frac{dT_m}{dt} = -\lambda T_m - \gamma(T_m - T_d) + F \tag{4}$$

$$C_d \frac{dT_d}{dt} = \gamma(T_m - T_d) \tag{5}$$

Parameters are traditionally estimated using individual equations, or calibrated based on theory or general circulation model (GCM) simulations. I show in section 4 that this system of differential equations in discrete time is mathematically equivalent to a cointegrated vector auto-regression which can be estimated using econometric techniques.

3 Cointegrated Vector Autoregressions

Econometric cointegration analysis can be used to overcome difficulties associated with stochastic trends in time series and applied to test whether there exist combinations of non-stationary series that are themselves stationary. To model both the short-run and long-run relations between non-stationary time series, I outline the structure of cointegrated vector auto-regressions (CVAR) in econometrics[3] and in the following section show the equivalence to the two-component energy balance model.

Let $\mathbf{Y}_t = (Y_{1,t}, Y_{2,t}, ..., Y_{p,t})'$ denote a p-dimensional vector of p non-stationary (specifically $I(1)$ or integrated of order one[4]) variables to be modelled for which observations are available over time. In equilibrium-correction form the CVAR model is given by:

$$\Delta \mathbf{Y}_t = \Gamma_1 \Delta \mathbf{Y}_{t-1} + ... + \Gamma_k \Delta \mathbf{Y}_{t-k} + \Pi \mathbf{Y}_{t-1} + \Phi + \boldsymbol{\epsilon}_t \tag{6}$$

[3]See Hendry & Juselius (2001), and Juselius (2006) for a comprehensive overview of cointegration methods.
[4]A series that is $I(s)$, or integrated of order $s > 0$, needs to be differenced s times to be stationary.

where Δ is the first difference operator, such that $\Delta Y_t = Y_t - Y_{t-1}$. The CVAR describes changes in the endogenous $\mathbf{Y}_t$ variables as a function of past changes up to k lags through the coefficient matrices Γ_1, Γ_k and changes in the long run-dynamics as captured through the coefficient matrix Π. The rank of Π determines the presence of cointegrating, or long-run, stationary relations. If the rank of $\Pi = 0$, there are no cointegrating relations, and if Π is full rank, the system must be stationary. The matrix Π will have full rank if the series tested are stationary ($\sim I(0)$) or if all endogenous stochastic trends can be explained by exogenous variables entering the cointegrating relation. The matrix has a rank of zero if the series do not cointegrate, and reduced rank ($p > r > 0$) if the series cointegrate. The number of cointegrating relations is chosen using the trace statistic which tests the null hypothesis that there are $r-1$ cointegrating relations against the null hypothesis that there are r relations (Johansen 1988, Johansen 1995). To alleviate concerns associated with small samples, a bootstrapping procedure to test the cointegrating rank (see Cavaliere et al. 2012) could be used. Using a system approach (Johansen 1988) avoids many problems associated with single equation cointegration procedures (e.g. Engle & Granger 1987) and does not require pre-testing of the individual series for stationarity (for a discussion of potential hazards see Pretis & Hendry 2013).

In cointegration, the long-run dynamics are modelled explicitly by decomposing the estimated matrix Π under reduced rank into a cointegrating vector β and the adjustment coefficients α to this cointegrating vector:

$$\alpha\beta' = \Pi \tag{7}$$

It then holds that $\beta'\mathbf{Y_t}$ forms a stationary combination that describes the long-run dynamics between the endogenous variables. The elements of α describe how the individual variables adjust to this long-run relation.

Consider the case of three endogenous variables: $Y_{1,t}, Y_{2,t}, Y_{3,t}$ with a single lag in the CVAR specification where I have assumed for illustration purposes the presence of a single cointegrating relation (rank of $\Pi = 1$):

$$\begin{bmatrix}\Delta Y_{1,t}\\ \Delta Y_{2,t}\\ \Delta Y_{3,t}\end{bmatrix} = \mathbf{\Gamma} \cdot \begin{bmatrix}\Delta Y_{1,t-1}\\ \Delta Y_{2,t-1}\\ \Delta Y_{3,t-1}\end{bmatrix} + \begin{bmatrix}\alpha_1\\ \alpha_2\\ \alpha_3\end{bmatrix} \cdot \begin{bmatrix}\beta_1 & \beta_2 & \beta_3\end{bmatrix} \cdot \begin{bmatrix}Y_{1,t-1}\\ Y_{2,t-1}\\ Y_{3,t-1}\end{bmatrix} + \epsilon_t \tag{8}$$

The cointegrating relation is given by $\beta'\mathbf{Y}_{t-1}$ which is stationary. In equilibrium it holds that:

$$\beta'\mathbf{Y}_{t-1} = (\beta_1 Y_{1,t-1} + \beta_2 Y_{2,t-1} + \beta_3 Y_{3,t-1}) = 0 \tag{9}$$

If the expression is not in equilibrium, $\beta'\mathbf{Y}_{t-1} \neq 0$, then this disequilibrium moves the variables towards the new equilibrium through the adjustment coefficients $\alpha = (\alpha_1, \alpha_2, \alpha_3)'$.

4 Linking EBMs to Cointegration and Mapping to CVARs

I now show that the system of differential equations of the two-component EBM is equivalent to a restricted cointegrated system and can be mapped to a restricted CVAR. The energy balance

model in (4) and (5) can be expressed as

$$\frac{dT_m}{dt} = \frac{1}{C_m}\left[-\lambda T_m + F\right] + \frac{\gamma}{C_m}\left[T_m - T_d\right] \tag{10}$$

$$\frac{dT_d}{dt} = \frac{\gamma}{C_d}\left[T_m - T_d\right] \tag{11}$$

with no explicit formulation given for the changes in radiative forcing $\frac{dF}{dt}$ in the EBM. Let α and β denote $(p \times r)$ matrices (where $p = 3, r = 2$) corresponding to:

$$\alpha = \begin{bmatrix} \frac{1}{C_m} & \frac{\gamma}{C_m} \\ 0 & \gamma \\ 0 & 0 \end{bmatrix} \text{ and } \beta' = (\beta_1, \beta_2)' = \begin{bmatrix} -\lambda & 0 & 1 \\ 1 & -1 & 0 \end{bmatrix} \tag{12}$$

Then the two-component EBM can be written as the following system:

$$d\mathbf{Y} = \alpha\beta'\mathbf{Y}dt \tag{13}$$

where $\mathbf{Y} = (T_m, T_d, F)'$, a $(3 \times 1$ vector).

Assuming stochastic processes (e.g. due to imperfect measurement and omitted variables) the two component EBM can be written with a noise term $\mathbf{v}$ as an Ornstein-Uhlenbeck process given by the stochastic differential equation:

$$d\mathbf{Y} = \Pi\mathbf{Y}dt + \mathbf{v} \tag{14}$$

$$= \alpha\beta'\mathbf{Y}dt + \mathbf{v} \tag{15}$$

where Π is a $(p \times p)$ matrix of reduced rank $r = 2$ such that $\Pi = \alpha\beta'$. The noise term $\mathbf{v} = \mathbf{D}d\mathbf{W}$ captures omitted effects from the model, with $\mathbf{D}$ being a $(p \times p)$ matrix and $\mathbf{W}$ a p-dimensional Brownian motion. The following analysis relies on the results in Kessler & Rahbek (2004) and Kessler & Rahbek (2001).

The formulation of the stochastic two-component energy balance model then implies that, if the continuous Ornstein-Uhlenbeck process is integrated of order one, $I(1)$, the series in the EBM cointegrate into two stationary relations given by $\beta'\mathbf{Y}$ with adjustment coefficients of α. The physical stochastic two-component energy balance model is equivalent to a restricted cointegrated system in continuous time in (16) and (17) where the expressions in brackets correspond to the cointegrating vectors, and the coefficients outside the brackets are the α adjustment coefficients in the cointegration model:

$$\frac{dT_m}{dt} = \underbrace{\frac{1}{C_m}}_{\alpha_{1,1}} \underbrace{\left[-\lambda T_m + F\right]}_{\beta_1'\mathbf{Y}} + \underbrace{\frac{\gamma}{C_m}}_{\alpha_{1,2}} \underbrace{\left[T_m - T_d\right]}_{\beta_2'\mathbf{Y}} + v_{1,t} \tag{16}$$

$$\frac{dT_d}{dt} = \underbrace{\frac{\gamma}{C_d}}_{\alpha_{2,2}} \underbrace{\left[T_m - T_d\right]}_{\beta_2'\mathbf{Y}} + v_{2,t} \tag{17}$$

The energy balance model implies that the three variables of upper component temperatures, lower component temperatures, and radiative forcing cointegrate into two stationary relations. The first $\left(\beta_1'\mathbf{Y} = [-\lambda T_m + F]\right)$, an equation linking upper component temperatures to radiative forcing, describes the net heat flux (Q). The second $\left(\beta_2'\mathbf{Y} = [T_m - T_d]\right)$ is an equation describing the heat transfer between the upper and lower component. Upper component temperatures adjust to both cointegrating vectors, lower component temperatures adjust to the second cointegrating vector ($\alpha_{2,1} = 0$), and radiative forcing is weakly exogenous ($\alpha_{3,1} = \alpha_{3,2} = 0$). Cointegration between these variables is a testable property, and cointegration analysis can further be used to estimate and conduct inference on the parameters α and β.

The differential equations describe the two-component energy balance model in continuous time, while sampling happens at discrete intervals. Inference on cointegration and parameter estimates in the continuous-time EBM can be conducted based on discrete observations using the results in Kessler & Rahbek (2004).[5] It is important to note though that the discretization method moving from discrete to continuous time can have effects on the auto-correlation structure of the error term, and thus affect the statistical properties of the estimates (Sargan 1974). Given the specification in equation (15) as an Ornstein-Uhlenbeck process, discrete observations $\mathbf{Y}_t$ of $\mathbf{Y}$ follow a VAR process as in equation (18):

$$\mathbf{Y}_t = \mathbf{A}\mathbf{Y}_{t-1} + \boldsymbol{\epsilon}_\mathbf{t} \tag{18}$$

where $\boldsymbol{\epsilon}_t \sim N(\mathbf{0}, \boldsymbol{\Sigma})$. The coefficient matrix $\mathbf{A}$ in the VAR in (18) equals the matrix exponential of the coefficient matrix Π in equation (15), $\mathbf{A} = \exp(\Pi)$. This result derives from solving the Ornstein-Uhlenbeck process[6] in equation (15) – see appendix 7.1. Let $\mathbf{P} = \mathbf{A} - \mathbf{I}$, then (18) can be written in equilibrium correction form as:

$$\Delta\mathbf{Y}_t = \mathbf{P}\mathbf{Y}_t + \boldsymbol{\epsilon}_t \tag{19}$$

There is then a direct mapping of the EBM parameters from equation (15) to the parameters in the discrete-time model (19). In particular, the coefficient matrix $\mathbf{P}$ in the CVAR relates to the EBM parameters α, β as:

$$\mathbf{P} = \mathbf{A} - \mathbf{I} = \exp(\Pi) - \mathbf{I} = \exp\left(\alpha\beta'\right) - \mathbf{I} = \alpha\kappa\beta' = \tilde{\alpha}\beta' \tag{20}$$

where $\tilde{\alpha} = \alpha\kappa$ and the $(r \times r)$ matrix $\kappa = \left(\beta'\alpha\right)^{-1}\left[\exp\left(\beta'\alpha\right) - \mathbf{I}\right]$, see appendix 7.1 for a proof. This mapping implies that the two-component continuous-time EBM can be tested and estimated using a CVAR estimated on discrete observations: the rank of the coefficient matrix of the discrete-time VAR model equals that of the EBM, $\text{rank}(\mathbf{P}) = \text{rank}(\Pi) = \text{rank}(\alpha\beta')$, and the matrix $\widehat{\mathbf{P}} = \hat{\tilde{\alpha}}\hat{\beta}'$ yields estimates of the EBM parameters given by β'. The adjustment coefficients α are not identified given that the CVAR parameters $\tilde{\alpha}$ correspond to $\alpha\kappa$. Thus, restrictions in α are not directly preserved in the CVAR formulation. In other words, while in the continuous time EBM the lower component temperatures T_d do not adjust to the first

[5] In particular, Theorem 1 in Kessler & Rahbek (2004).

[6] Where for simplicity the frequency of observations is assumed to be equal to one.

cointegrating vector, $\alpha_{2,1} = 0$, this does not directly imply that the same holds for the discrete-time CVAR, $\tilde{\alpha}_{2,1} \neq 0$. An intuitive explanation for this comes from the fact that at the discrete time interval the lower component may adjust to the upper component given the feedback between T_m and T_d. The extent of this can be tested by assessing whether $\tilde{\alpha}_{2,1}$ equals zero or not using CVAR estimates.[7] One exception on restrictions linking α and $\tilde{\alpha}$ occurs under weak-exogeneity. The forcing series is assumed to be weakly-exogenous (not adjusting to the cointegrating relations) in the EBM, thus $\alpha_{3,1} = \alpha_{3,2} = 0$. Given $\tilde{\alpha} = \alpha\kappa$ this implies that $\tilde{\alpha}_{3,1} = \tilde{\alpha}_{3,2} = 0$, forcing should also be weakly exogenous in the CVAR formulation. Writing the model (19) in matrix form we can formulate equations (16) and (17) as a discrete CVAR where the CVAR parameters (given by $\tilde{\alpha}$ and β) correspond to (combinations of) parameters of the EBM:

$$\begin{bmatrix} \Delta T_{m,t} \\ \Delta T_{d,t} \\ \Delta F_t \end{bmatrix} = \begin{bmatrix} \tilde{\alpha}_{1,1} \\ \tilde{\alpha}_{2,1} \\ \tilde{\alpha}_{3,1} \end{bmatrix} \cdot \begin{bmatrix} \beta_{1,1} & \beta_{1,2} & \beta_{1,3} \end{bmatrix} \cdot \begin{bmatrix} T_{m,t-1} \\ T_{d,t-1} \\ F_{t-1} \end{bmatrix} \tag{21}$$

$$+ \begin{bmatrix} \tilde{\alpha}_{1,2} \\ \tilde{\alpha}_{2,2} \\ \tilde{\alpha}_{3,2} \end{bmatrix} \cdot \begin{bmatrix} \beta_{2,1} & \beta_{2,2} & \beta_{2,3} \end{bmatrix} \cdot \begin{bmatrix} T_{m,t-1} \\ T_{d,t-1} \\ F_{t-1} \end{bmatrix} + \boldsymbol{\epsilon}_t \tag{22}$$

The cointegrating vectors and adjustment coefficients are linked to the continuous-time two-component EBM such that: $\beta_{1,1} = -\lambda, \beta_{1,2} = 0, \beta_{1,3} = 1$, linking upper component temperatures and radiative forcing in the first cointegrating relation; $\beta_{2,1} = -\beta_{2,2} = 1$, and $\beta_{2,3} = 0$, linking upper component temperatures and lower component temperatures in the second cointegrating relation; and $\tilde{\alpha}_{3,1} = \tilde{\alpha}_{3,2} = 0$, as forcing is assumed to adjust to neither cointegrating relation. In matrix notation this can be expressed as:

$$\begin{bmatrix} \Delta T_{m,t} \\ \Delta T_{d,t} \\ \Delta F_t \end{bmatrix} = \begin{bmatrix} \tilde{\alpha}_{1,1} \\ \tilde{\alpha}_{2,1} \\ 0 \end{bmatrix} \cdot \begin{bmatrix} -\lambda & 0 & 1 \end{bmatrix} \cdot \begin{bmatrix} T_{m,t-1} \\ T_{d,t-1} \\ F_{t-1} \end{bmatrix} \tag{23}$$

$$+ \begin{bmatrix} \tilde{\alpha}_{1,2} \\ \tilde{\alpha}_{2,2} \\ 0 \end{bmatrix} \cdot \begin{bmatrix} 1 & -1 & 0 \end{bmatrix} \cdot \begin{bmatrix} T_{m,t-1} \\ T_{d,t-1} \\ F_{t-1} \end{bmatrix} + \boldsymbol{\epsilon}_t$$

This yields the discrete-time CVAR representation of the stochastic energy balance model and can be estimated using standard CVAR methods.

4.1 Testable Properties implied by the EBM-CVAR mapping

The equivalence of a two component EBM and a CVAR provides direct restrictions which can be tested against observations. Formally the EBM implies the following properties of the estimated CVAR (6) which can then be tested:

1. rank(Π)=2: the time series cointegrate to two stationary relations, linking upper compo-

[7] Section 5 investigate this further.

nent temperatures with radiative forcing, and lower component temperatures with upper component temperatures (trace test).

2. Restrictions in (23) are not rejected (Likelihood ratio test).

3. Estimates for β (and $\tilde{\alpha}$) are statistically different from zero, (Likelihood ratio tests) and theory-consistent.

In particular, for the EBM to hold we require that the three series – upper component temperatures, lower component temperatures, and radiative forcing – cointegrate into two stationary relations: The first, an equation linking upper component temperatures to radiative forcing, describing the net heat flux (Q):

$$h_{1,t} = \left(\beta_{1,1} T_{m,t-1} + \beta_{1,3} F_{t-1}\right) \tag{24}$$

where $\beta_{1,1} = -\lambda$, and $\beta_{1,3} = 1$. The second, an equation describing the heat transfer between the upper and lower component:

$$h_{2,t} = \left(\beta_{2,1} T_{m,t-1} + \beta_{2,2} T_{d,t-1}\right) \tag{25}$$

where $\beta_{2,1} = 1 = -\beta_{2,2}$. The order of cointegration, can be tested using the Johansen trace test (Johansen 1988).

With respect to the physical structure between variables, this implies that any stochastic trends present in the radiative forcing (where the stochastic component is driven by anthropogenic emission of greenhouse gases from stochastic economic activity) will be imparted onto the temperatures of the mixed component, through which it transfers onto the lower component. This generalizes the results in Kaufmann et al. (2013) to the two-component EBM.

Notably, estimating a two-component EBM through a CVAR avoids potential hazards associated with statistical and econometric climate models. The Johansen cointegration procedure requires no pre-testing of individual series for the order integration (up to I(1)) and takes the system nature of the model into account. The model also relies on the aggregate of radiative forcing, rather than single series which, individually, may suffer from data measurement problems.

The CVAR modelling approach provides the foundations for coupling empirical EBMs with models of the macroeconomy by expanding the system in (6) using an explicit formulation for the forcing series F_t. The forcing can be disaggregated into natural and anthropogenic factors, where concentrations of greenhouse gases are modelled as the accumulation of emissions driven by economic activity and social changes. Feedbacks of climate variables onto economic variables can then be estimated in the CVAR formulation yielding estimates of damages and the social cost of carbon.

4.2 Estimation using ocean heat content observations

The EBM characterises changes in temperatures while the data available for applications often is a mixture of heat content and temperature observations. Given the availability of data, the

application in section 5 uses ocean heat content (H_t) for the lower component and temperatures for the upper component. This transformation yields a re-parametrised, but otherwise identical EBM for estimation, where I use $H_t \approx C_d T_{d,t}$, the re-parametrised EBM is given as:

$$\begin{bmatrix} \Delta T_{m,t} \\ \Delta H_{,t} \\ \Delta F_t \end{bmatrix} = \begin{bmatrix} \tilde{\alpha}_{1,1} \\ \tilde{\alpha}_{2,1} \\ 0 \end{bmatrix} \cdot \begin{bmatrix} -\lambda & 0 & 1 \end{bmatrix} \cdot \begin{bmatrix} T_{m,t-1} \\ H_{t-1} \\ F_{t-1} \end{bmatrix} + \begin{bmatrix} \tilde{\alpha}_{1,2} \\ \tilde{\alpha}_{2,2} \\ 0 \end{bmatrix} \cdot \begin{bmatrix} 1 & -1/C_d & 0 \end{bmatrix} \cdot \begin{bmatrix} T_{m,t-1} \\ H_{t-1} \\ F_{t-1} \end{bmatrix} + \boldsymbol{\epsilon}_t \tag{26}$$

To determine the cointegrating rank of the model, estimation includes an unrestricted constant.[8] If the rank equals two, then the first corresponding cointegrating vector is restricted and given by:

$$h_{1,t} = \left(\beta_{1,1} T_{m,t-1} + \beta_{1,3} F_{t-1}\right) \tag{27}$$

The second, a restricted equation for temperature changes in the lower component:

$$h_{2,t} = \left(\beta_{2,1} T_{m,t-1} + \beta_{2,2} H_{t-1}\right) \tag{28}$$

For identification both cointegrating vectors are normalized such that $\beta_{1,3} = 1$ and $\beta_{2,1} = 1$. The additional restrictions given by the EBM are: lower component temperatures do not enter the first cointegrating vector, $\beta_{1,2} = 0$; radiative forcing does not enter the second cointegrating vector, $\beta_{2,3} = 0$, and is weakly exogenous, $\alpha_{3,1} = \alpha_{3,2} = 0$ which implies that $\tilde{\alpha}_{3,1} = \tilde{\alpha}_{3,2} = 0$. This is a simplification since some of the radiative forcing series are determined endogenously, CO_2 concentrations generally vary with temperatures as does ice-albedo. The weak exogeneity assumption is relaxed in a simple extension of the model (see model C in Table 2) where an aggregate of radiative forcing is modelled endogenously.

Every parameter in the cointegrating vector of the CVAR has a structural interpretation. To estimate the model parameters of interest, it then holds that in the second cointegrating vector (28) $\beta_{2,2} = -1/C_d$, providing an estimate of the heat capacity of the deep component. The climate feedback parameter λ can be determined using $\beta_{1,1} = -\lambda$. Approximate standard errors and confidence intervals can be derived using the asymptotic normality of the cointegrating parameters. In the case of parameters of interest being non-linear transformations of the cointegrating estimates (such as $-1/C_d = \beta_{1,1}$), I rely on the δ-method to provide approximate standard errors.[9] Based on these restrictions all EBM parameters in the approximation can be identified and the over-identifying restrictions can be tested.

[8] This allows for potential linear trends in the data, but no deterministic trends in the cointegration relations (see Hendry & Juselius 2001).

[9] Given an asymptotically normally distributed random variable X satisfying $\sqrt{n}(X - \mu) \xrightarrow{D} N\left(0, \sigma^2\right)$ and a continuous function $g(\mu)$, using a Taylor-expansion we can approximate the distribution of $g(X)$ by $\sqrt{n}\left(g(X) - g(\mu)\right) \xrightarrow{D} N\left(0, \sigma^2[g'(\mu)]^2\right)$.

5 Application

Here I estimate a CVAR as a simple test of the two-component EBM, and to obtain estimates of the model parameters, notably estimated climate sensitivity to empirically determine the response to a doubling of emissions, while accounting for the non-stationary nature of the climate time series. Future work will extend the system to endogenously model forcing by coupling the CVAR EBM to a model of macroeconomic time series.

5.1 Data

The upper/mixed component is specified as the atmosphere at the surface and temperatures are taken as global mean surface temperature anomalies from the GISS dataset (Hansen et al. 2010). The lower component is proxied by the ocean heat content anomalies from 0-700m (Levitus et al. 2009). This is a crude approximation as it omits the deep ocean and will therefore provide a high estimate of the adjustment speed of this component.[10] The series are graphed in Figure 1. Radiative forcing time series (Figure 2) are taken from Meinshausen et al. (2011). The aggregate of the forcing used for the model includes well-mixed greenhouse gases (WMGHGs)[11] including CO_2, stratospheric water vapour (Str. H_2O), stratospheric ozone (O_3), black carbon, stratospheric aerosols, snow albedo changes, land use changes, indirect aerosol effects and reflective aerosols. The short time period from 1955-2010 masks the dramatic increase in radiative forcing stemming from WMGHGs since the late 19th century.

To directly estimate the parameters of the EBM here I rely on the aggregate of radiative forcing. An extension could consider disaggregates by separating out volcanic forcing in the form of stratospheric aerosols. Stern and Kaufmann (2014) test for links between individual forcing series and surface temperatures, further work could focus on more detailed models using individual forcing series found to be significant in Stern and Kaufmann (2014), while series with little impact (e.g. black carbon) could be omitted. Few econometric models accounting for non-stationarity in the form of stochastic trends also consider ocean heat content and thus the heat transfer between the atmosphere/top component and the ocean. Stern (2006) is a notable exception. Relative to Stern (2006) here I provide a direct link to the two component EBM and estimate the system jointly as a CVAR.

Data availability for ocean heat content constrains the sample to a period from 1955 onwards. The estimation period is then 1955-2011 at an annual frequency, resulting in T=56 observations. This time period, together with the use of an aggregate of radiative forcing rather than individual series, alleviates some concerns over measurement changes and the data quality of the radiative forcing series (see Pretis and Hendry 2013).

While the time series properties of radiative forcing series are heavily debated in the econometric literature (Kaufmann & Stern 2002, D. I. Stern & Kaufmann 2000, Beenstock et al. 2012, Pretis and Hendry 2013), the individual order of integration of these series is not directly

[10] Data for deeper ocean heat content for 0-2000m is available but only through pentadal averages (Levitus et al. 2012).

[11] The major gases grouped together as WMGHGs include CO_2, CH_4, N_2O, and SF_6 (Sulfur hexafluoride) and are combined due to their long lifetime and property that they are "well-mixed" – concentrations are at approximately the same level across the globe (Myhre et al., 2013).

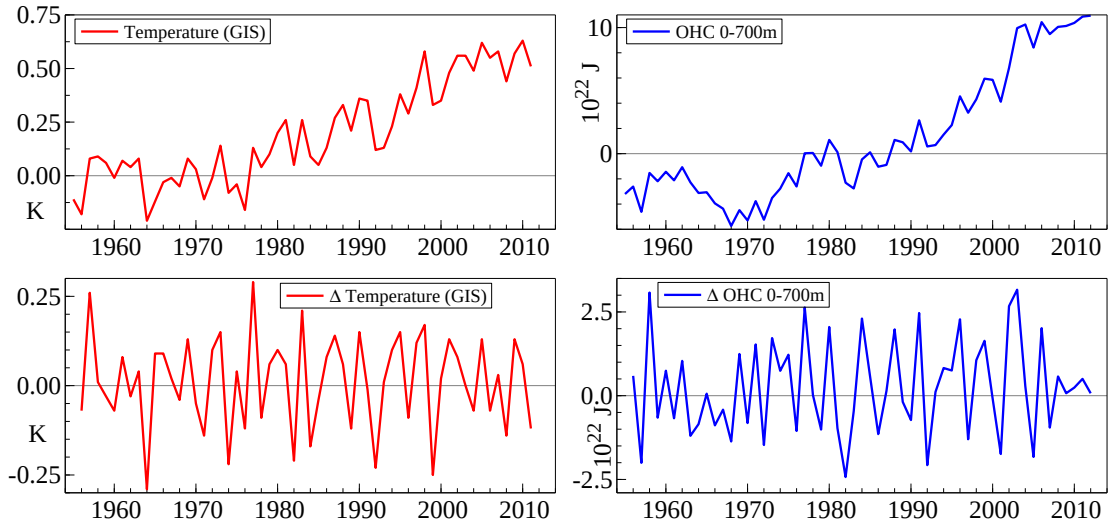

Figure 1: Left: Global mean surface temperatures in levels (top) and first differences (bottom). Right: Ocean heat content from 0-700m in levels (top) and first differences (bottom).

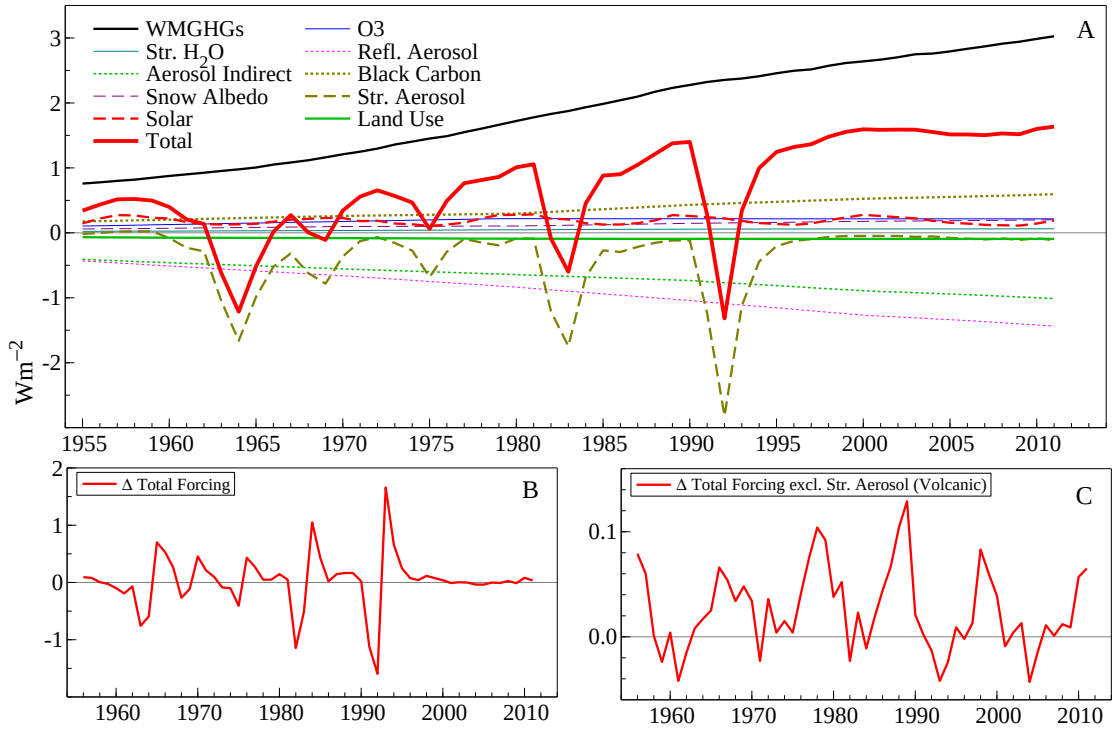

Figure 2: Radiative forcing from 1955-2011 in Wm^{-2}. Panel A shows disaggregated forcing, panel B shows the first difference of total forcing, panel C graphs first difference of total forcing excluding stratospheric aerosol forcing from volcanic eruptions. Data obtained from Meinshausen et al. (2011).

relevant. Within the EBM formulation it is aggregate forcing that drives upper component temperatures. On initial inspection it may appear inconsistent that global mean surface temperatures are well approximated by an $I(1)$ process while well-mixed greenhouse gases (in particular) atmospheric CO_2 concentrations can be argued to be $I(2)$ (see appendix section 7.6 and above sources). However, jointly the individual forcing series sum (or cointegrate) to an $I(1)$ aggregate of forcing, where the $I(1)$ cointegrating relation is given simply by the sum of the individual forcing series. Given the same unit of measurement and the aggregate effect, forcings are directly summable – this is a crucial oversight in the analysis of Beenstock et al. (2012) who argue that, due to the different time series properties, temperatures and WMGHGs cannot be related. While individual forcing series may be $I(2)$ or $I(0)$, aggregate forcing appears to be consistent with an $I(1)$ process, and thus exhibits approximately the same order of integration as global mean surface temperatures.[12]

5.2 Model Specification

Determining the number of cointegrating relations and conducting inference on the estimated parameters relies on well-specified models (Juselius 2006). While the theoretical EBM model does not imply additional lags, the time series properties of the data may support a longer lag length. To formally determine the lag structure I estimate a general unrestricted VAR starting with three lags. Removing the third lag is not rejected ($p = 0.08$), while dropping both the second and third lag is rejected ($p = 0.003$). The model with the lowest Schwarz criterion (Schwarz 1978) includes just one lag (SC=3.28, relative to 3.45 for two, and 3.76 for three lags). Assessing the diagnostic tests of the unrestricted models, a VAR(1) model rejects no-residual autocorrelation (p=0.003), while a VAR(2) passes the residual vector autocorrelation test (p=0.59) and dropping the second lag in the VAR(2) is rejected (p=0.005). Many discrete approximations use the average of two periods which further provides a justification for the use of two lags. Additional results on the dynamic stability and unit-root properties of the estimated VAR models are provided in appendix 7.2.

I proceed by estimating four variations of the CVAR EBM model. First, model A is estimated with a single lag corresponding to the theoretical two-component EBM. While this model is likely mis-specified and thus inference should be interpreted with care, it is included as a comparison to show the estimates if just the theory model is estimated. Second, model B includes two lags as suggested by the tests determining the lag structure. Once the restrictions implied by the EBM are imposed, both models A and B do not model forcing explicitly. Nevertheless, some of the forcing series are not exogenous but rather may vary with observed temperatures. Model C (estimated with 2 lags) relaxes the strong restrictions from model B by allowing aggregate forcing to adjust to the first cointegrating relation. This changes the system to three variables, however, no additional variables are included to explain forcing. In other words, radiative forcing is modelled endogenously and is allowed to adjust to the first cointegrating vector ($\tilde{\alpha}_{3,1} \neq 0$). Further research could expand the EBM to disaggregate the forcing

[12]While not required by the Johansen methodology, for completeness univariate unit root tests are provided in the appendix in section 7.6

series and also incorporate a macroeconomic VAR to model the anthropogenic emissions, as well as additional equations modelling natural variability (notably snow albedo changes).

An additional concern for residual autocorrelation are the time series properties of volcanic forcing (stratospheric aerosols) which act more as structural breaks than continuous series and may induce auto-correlation in the error terms. Therefore, a preliminary fourth specification, reported as Model V (in appendix 7.4) provides an initial attempt at modelling a simple disaggregate of the forcing series where volcanic aerosol forcing are modelled as breaks to avoid concerns of estimating climate sensitivities based on volcanic forcing in general (see e.g Lindzen & Giannitsis 1998). Only limited results are reported on model V as the precise modelling of volcanic eruptions requires a detailed treatment exceeding the scope of this paper in which the application to real data serves primarily as an illustration of estimating EBMs using CVARs.

In summary, model A corresponds directly to the EBM theory with a single lag, model B is estimated with two lags to account for additional dynamics and residual autocorrelation, model C is equivalent to model B with weak-exogeneity of the forcing series relaxed. Model V in appendix 7.4 provides an initial attempt at accounting for break-like volcanic forcing. Full results are reported for models A-C. Models are estimated using PcGive 14 (Doornik & Hendry 2013) and the *Ox* (Doornik 2009) programming language.

5.3 Results

The time series of global mean surface temperature anomalies, 0-700m ocean heat content anomalies, and total radiative forcing cointegrate to two stationary relations consistent with the theory of a two-component EBM. Likelihood ratio tests cannot reject the presence of two cointegrating vectors (rank = 2) in all the models estimated here (p_A=0.58, $p_B = p_C = 0.76$ for models A, B, C respectively), consistent with the theory provided by the two-component EBM (1). A single cointegrating relation (rank=1) is rejected in all models (see Table 1 for full results).[13]

Table 2 provides the estimated parameters of the CVAR. Fitted values are given in levels in Figure 3 and first differences in Figure 4. Residual plots are provided in appendix 7.5. The imposed restrictions on the CVAR are not rejected at the 1% level (p=0.02) in model A (see Table 2), though this should be interpreted with care given the failure of the residual autocorrelation mis-specification test of the model. The restrictions are, however, rejected in model B which controls for residual autocorrelation. To explore the rejection of the restrictions, model C relaxes weak-exogeneity of the forcing series. Taking into account the error serial correlation through the extension of the model to two lags, the model restrictions are not rejected in model C once forcing is allowed to adjust to upper component temperatures (p=0.32). This is a notably strong result – it is not unusual for restrictions of this complexity to be rejected.[14] For completeness, despite the rejection of the restrictions in model B and mis-specification in A, the proceeding analysis reports results for all models A, B, and C.

[13] Future work will explore the effects of the small sample sizes using the bootstrap rank testing approach in Cavaliere et al. 2012.

[14] Equally future work will explore the effects of the small sample sizes using the bootstrap hypotheses testing approach in Cavaliere et al. 2014.

Normality of the residuals cannot be rejected in diagnostic tests of the models A and B, it is, however, rejected for model C. The rejection of normality in C likely stems from the forcing series as indicated by the single-equation diagnostic tests – normality is not rejected in all but the forcing series. This can be driven by the volcanic impacts resembling structural breaks. Model V in (appendix 7.4), modelling volcanic forcing as breaks, shows improvements in diagnostic test results (see also the residual plots in appendix 7.5) and the EBM restrictions (including weak exogeneity of forcing) are then not rejected (p=0.17).

The estimated parameters of the EBM in the cointegrating relations are highly significant and estimated with theory-consistent signs. There is little evidence that the ocean heat content series adjusts to the first cointegrating vector ($\tilde{\alpha}_{2,1}$ is insignificant in Table 2).[15] This is consistent with the continuous-time EBM where the lower component only adjusts to the second cointegrating relation in (17).The two cointegrating relations representing the equations of the EBM are reported here as an example for the EBM theory model A:

$$\widehat{h}_{1,t} = \left(\underset{(0.51)**}{-\,2.71}\; T_{m,t-1} + F_{t-1} \right) \tag{29}$$

$$\widehat{h}_{2,t} = \left(T_{m,t-1} - \underset{(0.003)**}{0.044}\; H_{t-1} \right) \tag{30}$$

where standard errors are given in parentheses and the coefficients on F_{t-1} in the first equation, and the coefficient on $T_{m,t-1}$ in the second equation are normalized to 1 for identification.

Table 1: Cointegration Tests of the Two-Component EBM

	A: Base, 1-lag	**B & C: 2-lag**
Rank=0	61.52 [p <0.00]**	57.90 [p <0.00]**
Rank=1	20.35 [p <0.01]**	22.46 [p <0.01]**
Rank=2	0.31 [p=0.58]	0.09 [p=0.76]
Obs.	56	55

Cointegration rank tests using the Johansen (1988) trace test. p-values are reported in brackets [ ], * indicates rejection at 5%, ** indicates rejection at 1%.

[15] Further discussion of estimated model parameters is provided in appendix 7.3.

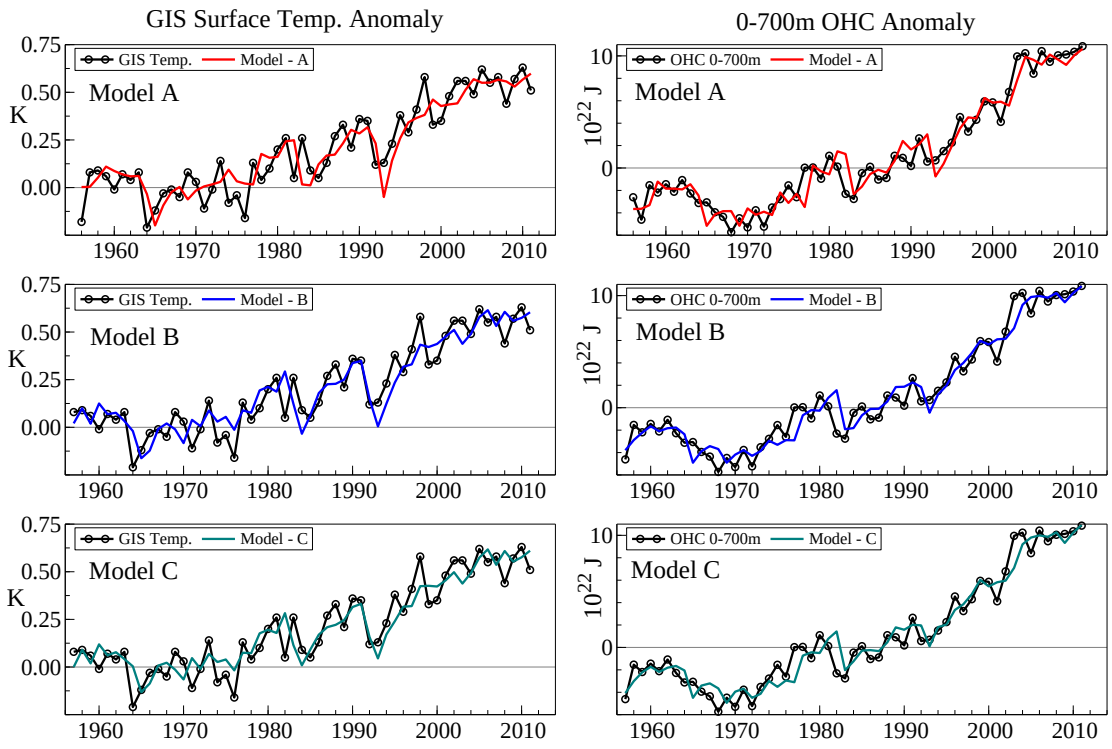

Figure 3: EBM Model Fit (estimated as a CVAR). Left panels shows model fit and observed (GIS) upper-component (global mean-surface) temperature anomalies. Right panels shows model fit and observed 0-700m ocean heat content (OHC) anomalies (Levitus et al. 2009) which proxy lower component heat content in the EBM.

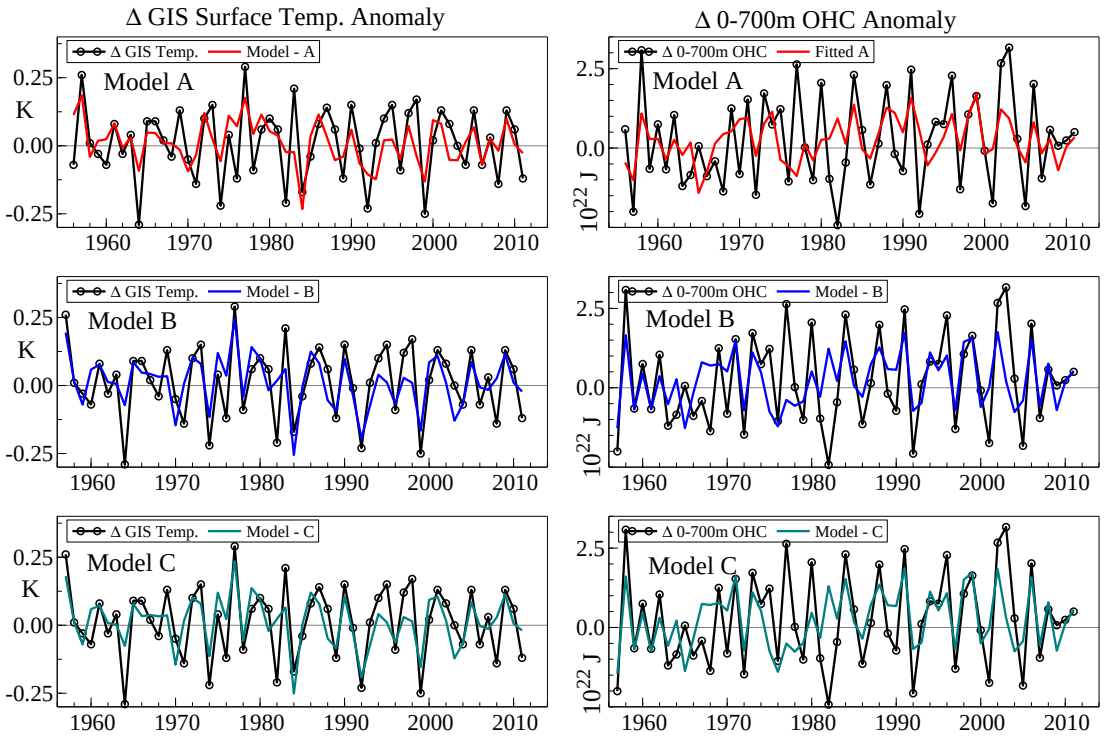

Figure 4: EBM Model Fit of First Differences (estimated as a CVAR). Left panels shows model fit and observed first differences of (GIS) upper-component (global mean-surface) temperature anomalies. Right panels shows model fit and first differences of observed 0-700m ocean heat content anomalies (Levitus et al. 2009) which proxy lower component heat content in the EBM.

Table 2: EBM Cointegration Model Parameter Estimates where $\tilde{\alpha} = \alpha\kappa$

	EBM/CVAR Model		
Coint. Relations	**A: Base**	**B: 2-lag**	**C: Endo. Forc.**
Vector 1 (Mixed)			
$\beta_{1,1}$	-2.71 (0.51)**	-2.29 (0.41)**	-2.21 (0.32)**
$\beta_{1,2}$	-	-	-
$\beta_{1,3}$	1	1	1
Adjustment			
$\tilde{\alpha}_{1,1}$	0.11 (0.03)**	0.15 (0.03)**	0.11 (0.03)**
$\tilde{\alpha}_{2,1}$	0.60 (0.33)	0.53 (0.38)	-0.03 (0.41)
$\tilde{\alpha}_{3,1}$	-	-	-0.55 (0.15)**
Vector 2 (Deep)			
$\beta_{2,1}$	1	1	1
$\beta_{2,2}$	-0.044 (0.003)**	-0.041 (0.004)**	-0.041 (0.004)**
Adjustment			
$\tilde{\alpha}_{1,2}$	-0.41 (0.12)**	-0.46 (0.15)**	-0.47 (0.15)**
$\tilde{\alpha}_{2,2}$	7.82 (1.48)**	7.43 (1.99)**	7.35 (1.99)**
$\tilde{\alpha}_{3,2}$	-	-	-
LR Test of Restric.			
$\chi^2(2)$, C: $\chi^2(1)$	12.87 [p=0.012]*	16.32 [p=0.003]**	2.47 [p=0.12]
Diagnostic Tests			
AR (1-2) F-Test	2.96 [p=0.005]**	1.32 [p=0.24]	1.14 [p=0.32]
Normality $\chi^2(4)$, C: $\chi^2(6)$	0.76 [p=0.94]	7.19 [p=0.13]	20.36 [p=0.002]**
Observations T	56	55	55
log-likelihood	-72.48	-59.85	-51.84
EBM Estimates			
λ (W$m^{-2}K^{-1}$)	2.71 (0.51)	2.29 (0.41)	2.21 (0.32)
ECS (K)	1.37 (0.25)†	1.62 (0.29)†	1.67 (0.24)†
C_m (W year $m^{-2}K^{-1}$)	-	-	-
C_d (W year $m^{-2}K^{-1}$)	22.72 (1.54)†	24.39 (2.38)†	24.39 (2.38)†
γ	-	-	-

Model estimates based on CVAR estimation. Standard errors are given in parentheses ( ) while p-values are reported in brackets [ ]. Standard errors are provided where available. If no standard errors are reported, then parameter is restricted or derived from estimated model parameters. * indicates significance at 5%, ** indicates significance at 1%. Standard errors derived using δ-method are marked using †. Left column specifies parameters, right columns shows estimation results. Dash - marks imposed restriction and no identification in the case of the structural EBM parameters given the theoretical result of $\tilde{\alpha} = \alpha\kappa$.

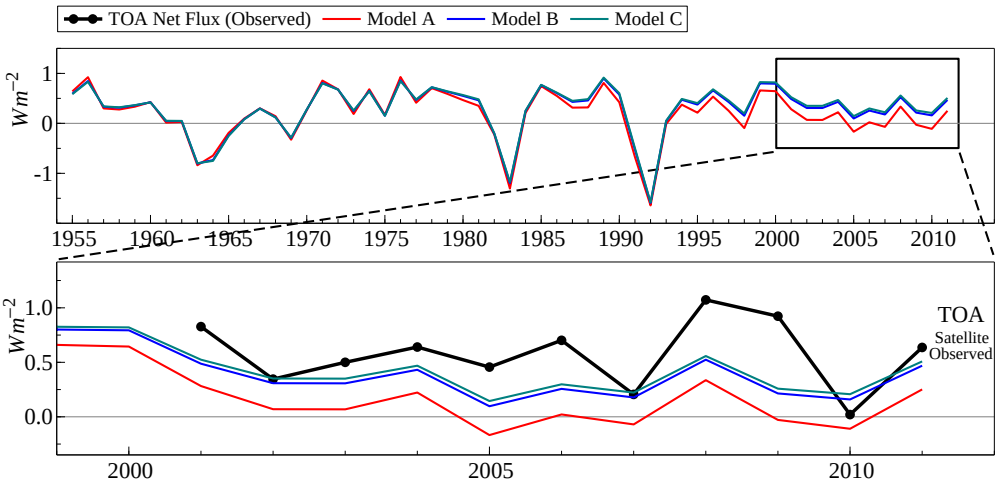

Figure 5: Net heat flux based on the first cointegrating vector and observed top of the atmosphere (TOA) net flux. Top panel graphs the net heat flux as described by the estimated first cointegrating vector for models A-C from 1955-2011. Bottom panel graphs the net flux from 2000-2011 together with annually averaged observed TOA net flux from the CERES Energy Balanced and Filled (EBAF) all skies data (black line with points) (Loeb et al. 2009) which have not been used to estimate the model and serve as an informal test of the model against a different set of independently measured observations.

5.4 Discussion

5.4.1 Physical Interpretation of First Cointegrating Vector

Based on the EBM in (1) and the equivalent cointegration formulation (24), the first cointegrating relation used to estimate climate feedback has a direct physical interpretation and describes the net heat flux or net energy coming into the system: $Q = F - \lambda T_m$. As an informal test of the model I compare the estimated cointegrating vector which corresponds to estimated net heat flux Q against the independently observed net heat flux from satellite-based measurements of annually averaged net flux at the top of the atmosphere (TOA) from the CERES Energy Balanced and Filled (EBAF) All Skies data (Loeb et al. 2009). It is important to emphasize that this data series is not used in the estimation of the model but is a different set of observations from satellite measurements of the quantity captured by the first cointegrating relation. Figure 5 plots the first cointegrating relation together with the satellite measurements. While the models under-estimate the volatility and level slightly, the first cointegrating vectors from models B and C remain close to the satellite-observed record. Model A, which does not control for residual autocorrelation (and results in high estimates of climate feedback – see section 5.4.2), consistently lies below satellite-observed TOA net flux.

5.4.2 Climate Feedback and Sensitivity

The system's response to an increase in emissions is crucial for climate policy and assessment of future damages. The estimates of the climate response to increasing emissions is characterised by

climate feedback λ and the equilibrium climate sensitivity.[16] Estimates of climate feedback and equilbrium climate sensitivity (see Table 2) depend on the model specification, where model mis-specification likely leads to an over-estimation of climate feedback (and thus an under-estimation of climate sensitivity). Figure 6 plots the densities of estimated climate feedback (λ) and sensitivity (ECS) relying on approximate asymptotic normality.[17]

Using model A which does not control for residual-autocorrelation, λ is estimated to be 2.71 (0.51) $\mathrm{W}m^{-2}K^{-1}$, equivalent to an equilibrium climate sensitivity of 1.37 (0.25) K for a radiative forcing of $3.7Wm^{-2}$ for a step-shift doubling of CO_2. This is lower than IPCC (IPCC 2013) best estimates of around 3K. A possible reason for why climate feedback may have been over-estimated (and ECS under-estimated) when using observation-based approaches (for example Schwartz (2007) finds ECS for a doubling of CO_2 to be approximately 1.1K) could be model mis-specification (e.g apparent through residual autocorrelation) and stochastic trends in the data which are not accounted for when relying on correlations and not estimating the system as a whole. Equally, the standard errors are likely underestimated in the mis-specified models. Once residual autocorrelation is corrected for through the use of additional lags (model B) the estimates of climate feedback are lower (and those of ECS higher). Model B (two-lags) and model C (endogenous forcing) estimate λ at 2.29 (0.41) and 2.21 (0.32) $\mathrm{W}m^{-2}K^{-1}$ respectively, with associated equilibrium climate sensitivities of 1.62 (0.29) K and 1.67 (0.24) K. However, this should be interpreted with care as the now endogenous forcing is modelled as a simple aggregate.

There are concerns on estimating λ and ECS using volcanic forcing data (Lindzen & Giannitsis 1998). Model V makes an initial attempt in correcting for this by treating volcanic forcing as transitory breaks, entering the CVAR unrestrictedly in first differences. The climate feedback estimate in model V is notably lower than in models A-C, resulting in a higher estimate of ECS of 2.16 (0.56) K, however, associated with higher uncertainty (see Figure 6, model V, purple).

Overall, EBM estimates based on CVAR estimation show that the IPCC estimated range of equilibrium climate sensitivities is robust to the non-stationary nature of the data at hand, though at the higher end of the CVAR estimated distributions.

5.4.3 Stability and Time Dependence

Recursive Estimation The CVAR specification puts the entire econometric toolkit at the disposal of estimated EBMs and enables the stability of the model to be assessed over time using recursive estimation - I recursively estimate the model starting with a base sample of 20 observations from 1955-1976 onwards, expanding the sample up until 2011. This permits an assessment of how the estimates would have changed over time and can provide insight whether the recent slowdown in increase in surface temperatures – despite an increase in GHG concentrations (the "warming hiatus") – affects the estimates of the model parameters. Figure

[16] ECS for a doubling of CO_2 is derived from the steady-state equilibrium of the EBM. Using (4) and (5) in equilibrium it holds that $dT_m/dt = dT_d/dt = 0$ and thus $T_m = F/\lambda$. ECS is then defined as the equilibrium temperature response T_m given a radiative forcing of doubling of CO_2: ECS $= F_{2\times CO_2}/\lambda$, where $F_{2\times CO_2} \approx 3.7Wm^{-2}$.

[17] The results should be interpreted with care given the presence of residual autocorrelation in model A.

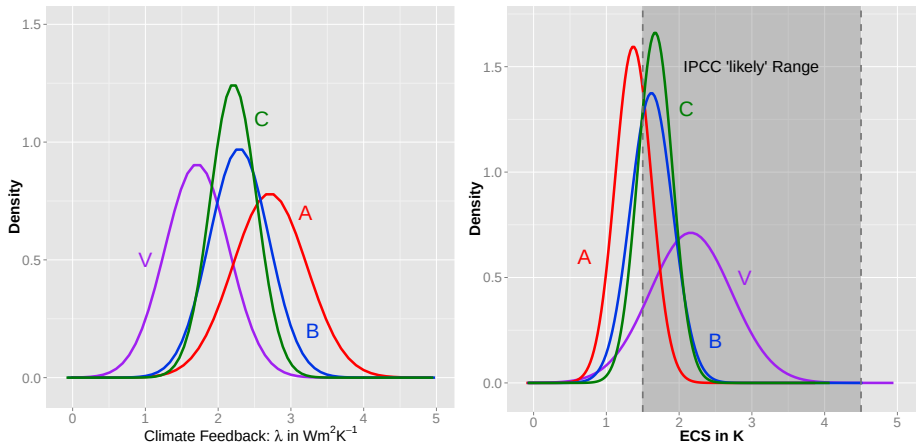

Figure 6: Estimated densities of climate feedback (λ, left) and equilibrium climate sensitivity (ECS, right), the equilibrium temperature response for a doubling of CO_2 for models A (theory), B (2-lags), and C (2-lags & endogenous forcing). Model V models volcanic forcing as breaks (see appendix 7.4). Densities are plotted based on the asymptotic normality of the CVAR parameter estimates. The IPCC "likely" range is denoted by vertical dashed lines in the right panel.

7 graphs the recursively estimated climate feedback and ECS over the sample period for the different model specifications. Consistent with the findings of Otto et al. (2013) (who use a single component EBM), the ECS and climate feedback are relatively stable over the sample prior to 2003. Notably, there is a dip in the recursively estimated system following 2003, where estimates including the time period thereafter yield a lower climate feedback and thus higher ECS with overall higher uncertainty as indicated by the $\pm$ 2 standard error interval.[18] This change in 2003 could be driven by sudden increased ocean heat uptake during this time period (see Figure 1).

The inclusion of the hiatus period (approximately from 1998 onwards), despite little increase in surface temperatures, suggests that estimates of ECS are relatively stable over time. This is likely driven by increased ocean heat uptake towards the end of the sample.

Ex-post 'forecasting' through the hiatus The cointegrated system model also provides a basis for making 'forecasts' and counter-factual policy analysis. As an illustration, to further investigate the performance and the stability of the EBM I re-estimate the models up until 1997 and forecast the remaining period (2011) 5-steps (years) ahead using the model estimates. While forecast performance is not a directly useful model evaluation tool (Clements & Hendry 2005), it can provide insights into model stability. The 5-step 'forecasts' used here rely on dynamic forecasting in a closed system – next period's forecast are used as starting points for succeeding forecasts up to five steps ahead (see e.g. Clements & Hendry 1999). Figure 8 graphs the 5-step 'forecasts' of the temperature and ocean heat content anomalies. While the forecast intervals are wide, the mean-level 'forecast' tracks observed temperatures and ocean heat content closely.

[18]The wide range of the $\pm$ 2 standard error interval for ECS in Figure 7 primarily stems from the non-linear transformation of the climate feedback estimate $\hat{\lambda}$. The estimate for λ in model B falls close to zero in 2001-2003 leading to very high values (and uncertainty) of ECS which is a non-linear transformation of λ.

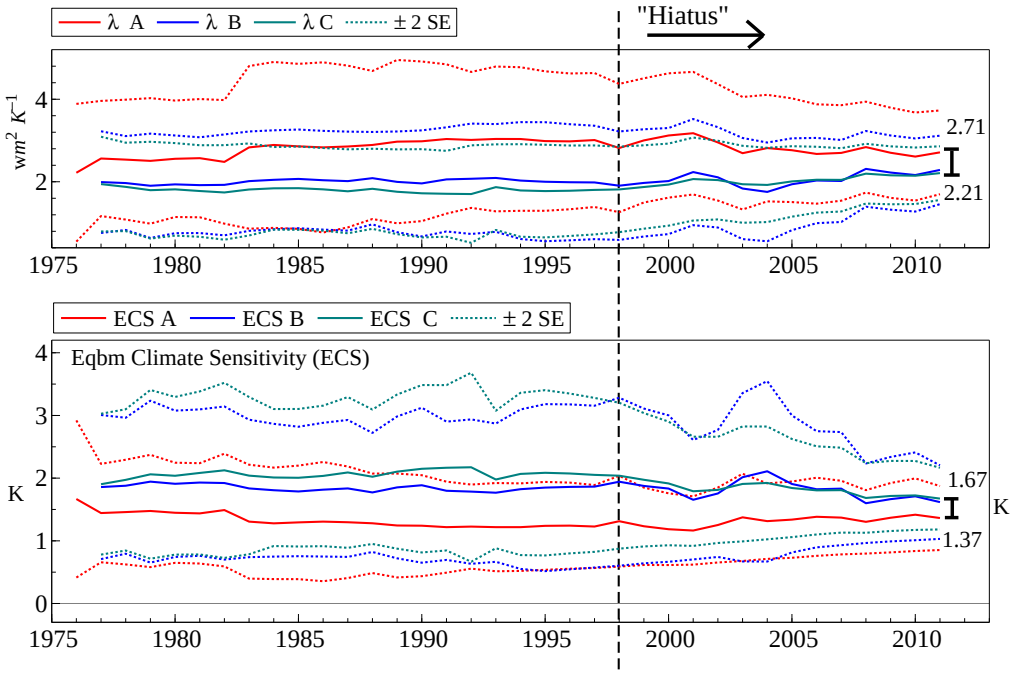

Figure 7: Recursive Estimates of Climate Feedback λ and Equilibrium Climate Sensitivity (ECS). Top panel shows the recursively estimated climate feedback λ starting with a base sample from 1956-1976 extended up to 1956-2011 for models A, B, and C. Bottom panel shows the corresponding ECS for a radiative forcing of 3.7 Wm^{-2} for a doubling of CO_2. Dashed lines graph the interval $\pm$ 2 standard errors, where standard errors for ECS are derived using the δ-method. While the $\pm$ 2 SE range is wide, the full sample 95% confidence interval is strictly positive for both ECS and λ. The range of full-sample point-estimates is denoted by black bars at the end of the sample.

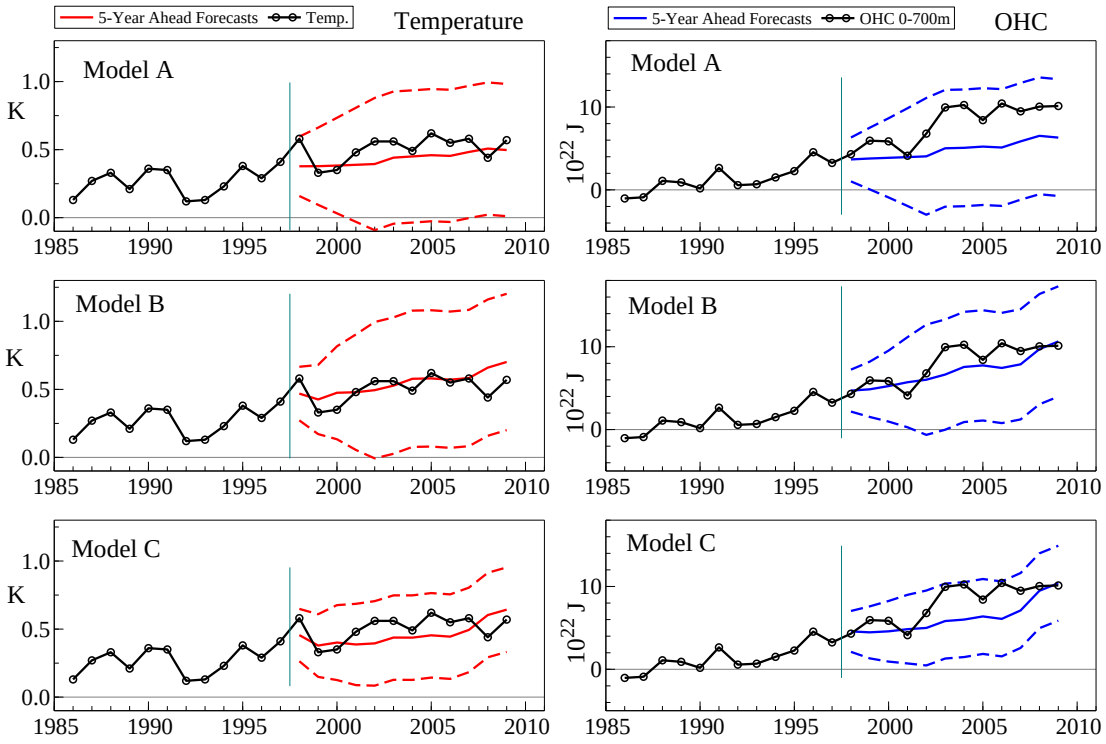

Figure 8: EBM/CVAR Model 5-Year Ahead Forecasts of Surface Temperature (left) and Ocean Heat Content (right) during the Hiatus for models A, B, and C.

This is consistent with Kaufmann et al. (2011): changes in radiative forcing over this time period together with ocean heat uptake can (in part) account for the slow down in warming. However, it appears that ocean heat uptake is generally slightly under-predicted relative to a model estimated prior to 1997. This may provide some evidence that increased ocean heat uptake accounts for some of the "missing energy" recently debated (Trenberth & Fasullo 2010, Trenberth & Fasullo 2012).

6 Conclusion

I demonstrate the mathematical equivalence of a two-component energy balance model to a cointegrated system that can be mapped to a cointegrated vector autoregression. This result provides directly testable properties of an energy balance model (EBM) when estimated on the observational record, while accounting for non-stationarity in the form of stochastic trends in the data. The equivalence result further provides a physical basis for the use of econometric cointegrated vector autoregressions (CVAR) in climate research, and places the entire toolkit of CVARs at the disposal of energy balance models, ranging from tests of stability, to forecasts. A simple application of econometric estimation of a two-component EBM using global mean surface temperature anomalies, 0-700m ocean heat content anomalies, and aggregates of radiative forcing suggests that the model is not rejected. The time series form two stationary relations (cointegrate), consistent with the theoretical model and individual parameters are

statistically significant with theory-consistent signs and magnitudes. CVAR estimation of a two-component EBM shows that estimates of equilibrium climate sensitivity are relatively stable over the sample of observations, where the recent slowdown in warming has little effect on the estimated climate sensitivity. However, careful thought has to be given how the radiative forcing series is modelled. Using the model parameter estimates, I find that model mis-specification (e.g. apparent through residual autocorrelation) results in high values of the observationally determined climate feedback, and in turn, to low estimates of equilibrium climate sensitivity.

This paper provides the foundation for the use of CVARs – which are commonly used to model the macroeconomy – in estimating econometric models consistent with physical laws. This will allow socio-economic models to be linked to climate models by estimating an entire system where the forcing series are endogenized and driven by economic activity. The feasibility of endogenously modelling a forcing series is demonstrated in Hendry & Pretis (2013). Using econometric methods to identify shifts in models (see e.g. Castle et al. 2015, Pretis et al. 2015, Pretis & Allen 2013) can then be used for an assessment of policy effectiveness and natural shocks. A system model that is consistent with physical laws may also permit feedbacks of temperatures and other climate variables onto the economy to be estimated as an alternative to calibrated measures of future damages and the social cost of carbon. This opens the door to data-driven models of interactions of the economy and climate.

References

Beenstock, M., Reingewertz, Y., & Paldor, N. (2012). Polynomial cointegration tests of anthropogenic impact on global warming. *Earth System Dynamics*, *3*(2), 173–188.

Castle, J. L., Doornik, J. A., Hendry, D. F., & Pretis, F. (2015). Detecting location shifts during model selection by step-indicator saturation. *Econometrics*, *3*(2), 240–264.

Cavaliere, G., Nielsen, B., Heino, & Rahbek, A. (2014). Bootstrap testing of hypotheses on co-integration relations in var models. *Econometrica*, *forthcoming*.

Cavaliere, G., Rahbek, A., & Taylor, A. (2012). Bootstrap determination of the co-integration rank in vector autoregressive models. *Econometrica*, *80*(4), 1721–1740.

Clements, M. P., & Hendry, D. F. (1999). *Forecasting non-stationary economic time series.* Cambridge, Mass.: MIT Press.

Clements, M. P., & Hendry, D. F. (2005). Evaluating a model by forecast performance. *Oxford Bulletin of Economics and Statistics*, *67*(s1), 931–956.

Dickey, D. A., & Fuller, W. A. (1981). Likelihood ratio statistics for autoregressive time series with a unit root. *Econometrica*, *49*, 1057–1072.

Doornik, J. A. (2009). An object-oriented matrix programming language Ox 6.

Doornik, J. A., & Hendry, D. (2013). *Pcgive 14.* London: Timberlake Consultants.

Engle, R. F., & Granger, C. W. J. (1987). Co-integration and error correction: Representation, estimation, and testing. *Econometrica*, *55:2*, 251-276.

Gregory, J., Stouffer, R., Raper, S., Stott, P., & Rayner, N. (2002). An observationally based estimate of the climate sensitivity. *Journal of Climate*, *15*(22), 3117–3121.

Hansen, J., Ruedy, R., Sato, M., & Lo, K. (2010). Global surface temperature change. *Reviews of Geophysics*, *48*(4), RG4004.

Held, I. M., Winton, M., Takahashi, K., Delworth, T., Zeng, F., & Vallis, G. K. (2010). Probing the fast and slow components of global warming by returning abruptly to preindustrial forcing. *Journal of Climate*, *23*(9), 2418–2427.

Hendry, D. F., & Juselius, K. (2001). Explaining cointegration analysis: Part II. *Energy Journal*, *22*, 75–120.

Hendry, D. F., & Pretis, F. (2013). Anthropogenic influences on atmospheric CO2. *Handbook on Energy and Climate Change*, 287.

IPCC. (2013). *Fith assessment report: Climate change 2013: Working Group I Report: The Physical Science Basis.* Geneva: IPCC. Retrieved from `https://www.ipcc.ch/report/ar5/wg1/`

Johansen, S. (1988). Statistical analysis of cointegration vectors. *Journal of economic dynamics and control*, *12*, 231-254.

Johansen, S. (1995). *Likelihood-based inference in cointegrated vector autoregressive models.* Oxford: Oxford University Press.

Juselius, K. (2006). *The cointegrated VAR model: Methodology and applications.* Oxford: Oxford University Press.

Juselius, K. (2011). Co-integration analysis of climate change: An exposition. *Working Paper*.

Kaufmann, R. K., & Juselius, K. (2013). Testing hypotheses about glacial cycles against the observational record. *Paleoceanography*, *28*(1), 175–184.

Kaufmann, R. K., Kauppi, H., Mann, M. L., & Stock, J. H. (2011). Reconciling anthropogenic climate change with observed temperature 1998–2008. *Proceedings of the National Academy of Sciences*, *108*(29), 11790–11793.

Kaufmann, R. K., Kauppi, H., Mann, M. L., & Stock, J. H. (2013). Does temperature contain a stochastic trend: linking statistical results to physical mechanisms. *Climatic change*, 1–15.

Kaufmann, R. K., & Stern, D. I. (2002). Cointegration analysis of hemispheric temperature relations. *Journal of Geophysical Research*, *107:2*.

Kessler, M., & Rahbek, A. (2001). Asymptotic likelihood based inference for co-integrated homogenous gaussian diffusions. *Scandinavian Journal of Statistics*, *28*(3), 455–470.

Kessler, M., & Rahbek, A. (2004). Identification and inference for multivariate cointegrated and ergodic gaussian diffusions. *Statistical inference for stochastic processes*, *7*(2), 137–151.

Levitus, S., Antonov, J., Boyer, T., Baranova, O., Garcia, H., Locarnini, R., ... others (2012). World ocean heat content and thermosteric sea level change (0–2000 m), 1955–2010. *Geophysical Research Letters*, *39*(10).

Levitus, S., Antonov, J., Boyer, T., Locarnini, R., Garcia, H., & Mishonov, A. (2009). Global ocean heat content 1955–2008 in light of recently revealed instrumentation problems. *Geophysical Research Letters*, *36*(7).

Lindzen, R. S., & Giannitsis, C. (1998). On the climatic implications of volcanic cooling. *Journal of Geophysical Research: Atmospheres (1984–2012)*, *103*(D6), 5929–5941.

Loeb, N. G., Wielicki, B. A., Doelling, D. R., Smith, G. L., Keyes, D. F., Kato, S., ... Wong, T. (2009). Toward optimal closure of the earth's top-of-atmosphere radiation budget. *Journal of Climate*, *22*(3).

Meehl, G. A., Arblaster, J. M., Fasullo, J. T., Hu, A., & Trenberth, K. E. (2011). Model-based evidence of deep-ocean heat uptake during surface-temperature hiatus periods. *Nature Climate Change*, *1*(7), 360–364.

Meinshausen, M., Smith, S. J., Calvin, K., Daniel, J. S., Kainuma, M., Lamarque, J., ... others (2011). The RCP greenhouse gas concentrations and their extensions from 1765 to 2300. *Climatic Change*, *109*(1-2), 213–241.

Myhre, G., Shindell, D., Breon, F., Collins, W., Fuglestvedt, J., Huang, J., ... Zhang, H. (2013). *Anthropogenic and natural radiative forcing* (Climate Change 2013: The Physical Science Basis. Contribution of Working Group I to the Fifth Assessment Report of the Intergovernmental Panel on Climate Change). Cambridge, UK: Cambridge University Press.

Otto, A., Otto, F. E., Boucher, O., Church, J., Hegerl, G., Forster, P. M., ... others (2013). Energy budget constraints on climate response. *Nature Geoscience*.

Pretis, F., & Allen, M. (2013). Climate science: Breaks in trends. *Nature Geoscience*, *6*, 992-993.

Pretis, F., & Hendry, D. (2013). Some hazards in econometric modelling of climate change. comment on" polynomial cointegration tests of anthropogenic impact on global warming" by beenstock et al.(2012). *Earth System Dynamics*, *4*(2), 375–384.

Pretis, F., Mann, M. L., & Kaufmann, R. K. (2015). Testing competing models of the temperature hiatus: assessing the effects of conditioning variables and temporal uncertainties through sample-wide break detection. *Climatic Change*, in-press, doi: 10.1007/s10584-015-1391-5.

Sargan, J. (1974). Some discrete approximations to continuous time stochastic models. *Journal of the Royal Statistical Society. Series B (Methodological)*, 74–90.

Schwartz, S. E. (2007). Heat capacity, time constant, and sensitivity of earth's climate system. *Journal of Geophysical Research*, *112*(D24), D24S05.

Schwartz, S. E. (2012). Determination of earth's transient and equilibrium climate sensitivities from observations over the twentieth century: strong dependence on assumed forcing. *Surveys in geophysics*, *33*(3-4), 745–777.

Schwarz, G. (1978). Estimating the dimension of a model. *Annals of Statistics*, *6*, 461–464.

Stern, D. I., & Kaufmann, R. K. (2000). Detecting a global warming signal in hemispheric temperature series: A structural time series analysis. *Climatic Change*, *47*, 411-438.

Stern, D. I., & Kaufmann, R. K. (2014). Anthropogenic and natural causes of climate change. *Climatic Change*, *122*(1-2), 257–269.

Stern, I., D. (2006). An atmosphere–ocean time series model of global climate change. *Computational statistics & data analysis*, *51*(2), 1330–1346.

Stern, N. (2013). The structure of economic modeling of the potential impacts of climate change: grafting gross underestimation of risk onto already narrow science models. *Journal of Economic Literature*, *51*(3), 838–859.

Trenberth, K. E., & Fasullo, J. T. (2010). Tracking earth's energy. *Science*, *328*(5976), 316–317.

Trenberth, K. E., & Fasullo, J. T. (2012). Tracking earth's energy: from El Niño to global warming. *Surveys in geophysics*, *33*(3-4), 413–426.

Watanabe, M., Kamae, Y., Yoshimori, M., Oka, A., Sato, M., Ishii, M., ... Kimoto, M. (2013). Strengthening of ocean heat uptake efficiency associated with the recent climate hiatus. *Geophysical Research Letters*.

7 Appendix

7.1 Further Results on the Continuous to Discrete Mapping

The energy balance model is given as:

$$d\mathbf{Y} = \Pi\mathbf{Y}dt + \mathbf{D}d\mathbf{W} \tag{31}$$

The solution to the Ornstein-Uhlenbeck process can be found using a change-of-variable approach. Define $\mathbf{Z}$ such that:

$$\mathbf{Z} = \exp(-\Pi t)\mathbf{Y} \tag{32}$$

where $\exp(-\Pi t)$ denotes the matrix exponential of $-\Pi t$, where for a $n \times n$ matrix $\mathbf{A}$ $\exp(\mathbf{A})$ is defined as:

$$\exp(\mathbf{A}) = \sum_{k=0}^{\infty} \frac{1}{k!}\mathbf{A}^k = \mathbf{I} + \mathbf{A} + \frac{1}{2!}\mathbf{A}^2 + \dots \tag{33}$$

with the inverse of $\exp(\mathbf{A})$ given by $\exp(\mathbf{A})^{-1} = \exp(-\mathbf{A})$. Pre-multiplying (32) by $\exp(\Pi t)^{-1}$ yields:

$$\mathbf{Y} = \exp(\Pi t)\mathbf{Z} \tag{34}$$

Using (32) we can write $d\mathbf{Z}$ as:

$$\begin{aligned} d\mathbf{Z} &= -\Pi\exp(-\Pi t)\mathbf{Y}dt + \exp(-\Pi t)d\mathbf{Y} && (35)\\ &= -\Pi\exp(-\Pi t)\mathbf{Y}dt + \exp(-\Pi t)(\Pi\mathbf{Y}dt + \mathbf{D}d\mathbf{W}) && (36)\\ &= \exp(-\Pi t)\mathbf{D}d\mathbf{W} && (37) \end{aligned}$$

Integrating from 0 to t yields:

$$\mathbf{Z} = \mathbf{Z}_0 + \int_0^t \exp(-\Pi u)\mathbf{D}d\mathbf{W}_u \tag{38}$$

Substituting for $\mathbf{Z}$ in (34) provides the solution to the Ornstein-Uhlenbeck process as:

$$\begin{aligned} \mathbf{Y} &= \exp(\Pi t)\mathbf{Y}_0 + \exp(\Pi t)\int_0^t \exp(-\Pi u)\mathbf{D}d\mathbf{W}_u && (39)\\ &= \exp(\Pi t)\left(\mathbf{Y}_0 + \int_0^t \exp(-\Pi u)\mathbf{D}d\mathbf{W}_u\right) && (40) \end{aligned}$$

Discrete observations $\mathbf{Y}_t$ of $\mathbf{Y}$ at a frequency of one then follow a VAR process as:

$$\mathbf{Y}_t = \mathbf{A}\mathbf{Y}_{t-1} + \boldsymbol{\epsilon}_\mathbf{t} \tag{41}$$

where $\mathbf{A} = \exp(\Pi)$, and $\boldsymbol{\epsilon}_t \sim N(\mathbf{0}, \boldsymbol{\Sigma})$. In equilibrium-correction form, the VAR is written as:

$$\Delta\mathbf{Y}_t = \mathbf{P}\mathbf{Y}_t + \boldsymbol{\epsilon}_t \tag{42}$$

with

$$\mathbf{P} = \mathbf{A} - \mathbf{I} = \exp(\Pi) - \mathbf{I} = \exp\left(\alpha\beta'\right) - \mathbf{I} = \alpha\kappa\beta' \tag{43}$$

where κ is a $(r \times r)$ matrix $\kappa = \left(\beta'\alpha\right)^{-1}\left[\exp\left(\beta'\alpha\right) - \mathbf{I}\right]$. Proof:

$$\begin{aligned}
\mathbf{P} &= \exp\left(\alpha\beta'\right) - \mathbf{I} \\
&= \mathbf{I} + \alpha\beta' + \alpha\beta'\alpha\beta'\frac{1}{2!} + \cdots - \mathbf{I} \\
&= \alpha\left(\mathbf{I} + \beta'\alpha\frac{1}{2!} + \ldots\right)\beta' \\
&= \alpha\left(\left(\beta'\alpha\right)^{-1}\left[\beta'\alpha + \beta'\alpha\beta'\alpha\frac{1}{2!} + \ldots\right]\right)\beta' \\
&= \alpha\left(\left(\beta'\alpha\right)^{-1}\left[\mathbf{I} + \beta'\alpha + \beta'\alpha\beta'\alpha\frac{1}{2!} + \cdots - \mathbf{I}\right]\right)\beta' \\
&= \alpha\left(\left(\beta'\alpha\right)^{-1}\left[\exp\left(\beta'\alpha\right) - \mathbf{I}\right]\right)\beta' \qquad (44)
\end{aligned}$$

For additional results see Kessler & Rahbek (2004).

7.2 Eigenvalues of the Companion Matrix

To further assess dynamic stability, Table 3 reports the moduli of the eigenvalues of the companion matrix of models A and B & C for the unrestricted VAR and reduced rank estimates (r=2) without the EBM theory restrictions imposed. The indicative results of the eigenvalue analysis suggest a single unit root: one eigenvalue lies on the unit circle, all other eigenvalues are within the unit circle. There is no evidence of an explosive process and the system does not appear to be $I(2)$ – once a reduced rank of two is imposed, all other eigenvalues are well within the unit circle.

Table 3: Eigenvalues of the companion matrix of models A and B & C for the unrestricted VAR and reduced rank (r=2) estimates (without EBM theory restrictions).

Model A (1 × 3 roots)			
VAR(1)	0.98	0.49	0.17
r=2	**1.00**	0.48	0.17

Models B & C (2 × 3 roots)						
VAR(2)	1.00	0.65	0.65	0.40	0.40	0.07
r=2	**1.00**	0.64	0.64	0.40	0.40	0.07

7.3 Estimates of Component Heat Capacity

While the upper-component heat capacity C_m (the amount of energy needed to change the temperature) is not directly identified in the discrete CVAR representation of the continuous-time EBM, the heat capacity of the lower component can be estimated using the parameters in the second cointegrating vector. The lower component heat capacity C_d is given by the CVAR mapping as $\beta_{2,2} = -1/C_d$. Raw estimates of the heat capacity of the lower component using observational data and a two-component EBM estimated as a CVAR from model A suggests an effective ocean 0-700m heat capacity of 22.72 (2.70) W year $m^{-2}K^{-1}$. This increases to 24.39 (2.38) when two lags are considered (models B) and when we allow forcing to be endogenous (Model C). Thus, when estimating the EBM as a system and taking the time series properties

into account, the raw estimate is higher than found by Schwartz (2012), who finds the heat capacity of the lower component up to 700m to be 14.1 W year $m^{-2}K^{-1}$ using OLS regression and suggests that his finding is a strong under-estimation. We may still under-estimate the total effective heat capacity of the system, mostly due to omission of the deeper ocean (>700m). Equally, other heat sinks are omitted in this simple model. If we follow Schwartz's approach of correcting the 0-700m estimate upwards (by 30% for deeper ocean, and 19% for other heat sinks), this yields an estimate of 36.34 W year $m^{-2}K^{-1}$ (using models B, C).

7.4 Modelling Volcanic Forcing as Breaks

Volcanic forcing ($F_{t,\text{Volc.}}$) closely resembles an impulse, where the first difference of volcanic forcing ($\Delta F_{t,\text{Volc.}}$) appears similar to a transitory shock dummy e.g. $(\dots, 0, 0, 1, -1, 0, 0, \dots)$ – see Figure 9 which plots the level and first difference of stratospheric aerosol (volcanic) forcing. This break-like behaviour likely drives the rejection of normality in Model C in section 5. There

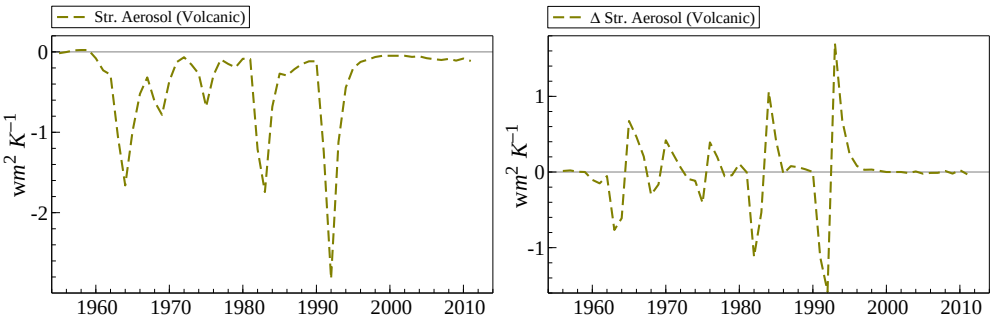

Figure 9: Radiative forcing of stratospheric aerosols from volcanic eruptions in levels, $F_{t,\text{Volc.}}$ (left) and first differences $\Delta F_{t,\text{Volc.}}$ (right)

are multiple different ways in which volcanic forcing can be modelled within the CVAR specification. The aggregate forcing series F_t could be disaggregated and separated into exogenous and endogenous forcing series, alternatively eruptions could be treated as transitory shocks. Here I follow the latter approach, future work will explore the modelling of eruptions within the CVAR in more detail.

Treating volcanic eruptions as closely resembling transitory breaks, I re-estimate the CVAR EBM from section 5 with 2-lags, where the forcing series $\tilde{F}_t = F_t - F_{t,\text{Volc.}}$ enters the first cointegrating relation, and is itself restricted to be weakly exogenous. The first difference of volcanic forcing, $\Delta F_{t,\text{Volc.}}$ enters the model unrestrictedly, similar to a transitory shock dummy.

Table 4 provides the estimation results where model V refers to the model including the first difference of volcanic forcing unrestrictedly. The model now passes the diagnostic tests for residual autocorrelation (p=0.21) and normality (p=0.22). The EBM restrictions, including weak-exogeneity of the remaining forcing series $\tilde{F}_t$, are not rejected (p=0.17). The estimate of ECS is notably higher relative to models A-C. Figure 6 in section 5 plots the approximate density of ECS and λ when estimated using model V.

Table 4: EBM Cointegration Model Parameter Estimates - Unrestricted Volcanic Forcing

	EBM/CVAR Model
Coint. Relations	**V: Volc. Breaks**
Vector 1 (Mixed)	
$\beta_{1,1}$	-1.71 (0.44)**
$\beta_{1,2}$	-
$\beta_{1,3}$	1
Adjustment	
$\tilde{\alpha}_{1,1}$	0.21 (0.06)**
$\tilde{\alpha}_{2,1}$	0.09 (0.81)
$\tilde{\alpha}_{3,1}$	-
Vector 2 (Deep)	
$\beta_{2,1}$	1
$\beta_{2,2}$	-0.042 (0.004)**
Adjustment	
$\tilde{\alpha}_{1,2}$	-0.65 (0.17)**
$\tilde{\alpha}_{2,2}$	6.43 (2.04)**
$\tilde{\alpha}_{3,2}$	-
LR Test of Restric.	
$\chi^2(2)$, C: $\chi^2(1)$	6.49 [p=0.17]
Diagnostic Tests	
AR (1-2) F-Test	1.37 [p=0.21]
Normality $\chi^2(4)$, C: $\chi^2(6)$	5.75 [p=0.22]
Observations T	55
log-likelihood	84.11
EBM Estimates	
λ (W$m^{-2}K^{-1}$)	1.71 (0.44)
ECS (K)	2.16 (0.56)†
C_m (W year $m^{-2}K^{-1}$)	-
C_d (W year $m^{-2}K^{-1}$)	23.8 (2.26)†
γ	-

Model estimates based on CVAR estimation. Standard errors are given in parentheses ( ) while p-values are reported in brackets [ ]. Standard errors are provided where available. If no standard errors are reported, then parameter is restricted or derived from estimated model parameters. * indicates significance at 5%, ** indicates significance at 1%. Standard errors derived using δ-method are marked using †. Left column specifies parameters, right columns shows estimation results. Dash - marks imposed restriction and no identification in the case of the structural EBM parameters given the theoretical result of $\tilde{\alpha} = \alpha\kappa$.

7.5 Residual Plots

Figure 10 plots the scaled model residuals from models A-C (see section 5) and model V (see section 7.4). The outlying observations in 1981/1982 are associated with strong volcanic forcing from the "El Chichón" eruption. Model V where volcanic forcing is modelled as transitory breaks alleviates some of these problems.

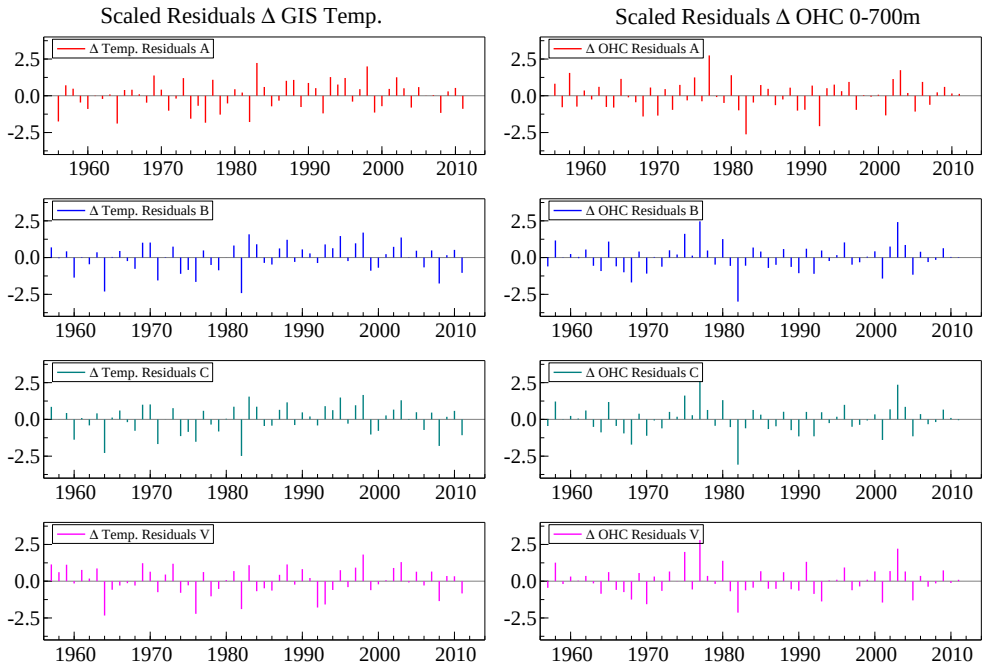

Figure 10: Scaled model residuals from models A-C (section 5) and model V (section 7.4)

7.6 Univariate Unit Root Tests

While the Johansen cointegration procedure does not require pre-testing for unit-roots, for completeness I provide the results of uni-variate augmented Dickey-Fuller (ADF) (Dickey & Fuller 1981) unit root tests on both levels and first differences for global mean surface temperatures, 0-700m ocean heat content, total radiative forcing, total radiative forcing excluding stratospheric aerosols (volcanic forcing) and well-mixed greenhouse gases (WMGHGs). The null hypothesis H_0 is that the series has a unit root, rejecting H_0 suggests no unit-root non-stationarity. D-lag specifies the number of lags included in the ADF test where choice of lag length is based on the lowest AIC. A constant is included in the ADF test specification. Test outcomes: ** indicates rejection of H_0 at 1% and * at 5%.

Table 5: GIS Temperature ADF Unit Root Tests

	GIS Temp.			Δ GIS Temp.	
D-Lag	**t-adf**	**AIC**	**D-Lag**	**t-adf**	**AIC**
3	-0.1707	-4.252	3	-4.329**	-4.263
2	-0.5416	-4.229	2	-6.850**	-4.291
1	-1.168	-4.161	1	-8.252**	-4.262
0	-1.949	-4.1	0	-10.26**	-4.172

Table 6: 0-700m OHC ADF Unit Root Tests

	0-700m OHC			Δ 0-700m OHC	
D-Lag	**t-adf**	**AIC**	**D-Lag**	**t-adf**	**AIC**
3	1.02	0.6989	3	-3.065*	0.6295
2	0.8619	0.6704	2	-5.301**	0.6821
1	0.3142	0.7122	1	-7.107**	0.6468
0	-0.1528	0.7377	0	-9.019**	0.675

Table 7: Total Radiative Forcing ADF Unit Root Tests

	Total Forcing			Δ Total Forcing	
D-Lag	**t-adf**	**AIC**	**D-Lag**	**t-adf**	**AIC**
3	-1.655	-1.476	3	-4.969**	-1.446
2	-1.789	-1.515	2	-5.400**	-1.457
1	-2.867	-1.454	1	-7.166**	-1.488
0	-2.299	-1.422	0	-6.182**	-1.335

Table 8: Total Forcing (excluding Stratospheric Aerosols) ADF Unit Root Tests

Total Forcing (excl. Str. Aerosols)			Δ Total Forcing (excl. Str. Aerosols)		
D-Lag	**t-adf**	**AIC**	**D-Lag**	**t-adf**	**AIC**
3	-0.5852	-6.789	3	-4.764**	-6.917
2	-0.7223	-6.763	2	-3.794**	-6.821
1	-0.7475	-6.801	1	-3.257*	-6.791
0	-0.7114	-6.43	0	-3.543*	-6.829

Table 9: Well-Mixed Greenhouse Gases (WMGHGs) ADF Unit Root Tests

WMGHGs			Δ WMGHGs		
D-Lag	**t-adf**	**AIC**	**D-Lag**	**t-adf**	**AIC**
3	-0.9117	-8.967	3	-1.793	-8.997
2	-0.6269	-8.902	2	-2.114	-8.989
1	-0.5831	-8.903	1	-2.898	-8.933
0	-0.6148	-8.619	0	-3.980**	-8.935